

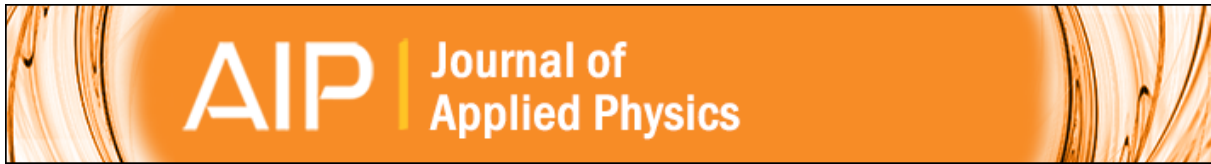


Strathprints Institutional Repository

Mathis, S. K. and Lau, K. H. A. and Andrews, A. M. and Hall, E. M. and Almuneau, G. and Hu, E. L. and Speck, J. S. (2001) *Lateral oxidation kinetics of AlAsSb and related alloys lattice matched to InP*. Journal of Applied Physics, 89. pp. 2458-2464. ISSN 0021-8979

Strathprints is designed to allow users to access the research output of the University of Strathclyde. Copyright © and Moral Rights for the papers on this site are retained by the individual authors and/or other copyright owners. You may not engage in further distribution of the material for any profitmaking activities or any commercial gain. You may freely distribute both the url (<http://strathprints.strath.ac.uk/>) and the content of this paper for research or study, educational, or not-for-profit purposes without prior permission or charge.

Any correspondence concerning this service should be sent to Strathprints administrator: <mailto:strathprints@strath.ac.uk>



Lateral oxidation kinetics of AlAsSb and related alloys lattice matched to InP

S. K. Mathis, K. H. A. Lau, A. M. Andrews, E. M. Hall, G. Almuneau, E. L. Hu, and J. S. Speck

Citation: *Journal of Applied Physics* **89**, 2458 (2001); doi: 10.1063/1.1335825

View online: <http://dx.doi.org/10.1063/1.1335825>

View Table of Contents: <http://scitation.aip.org/content/aip/journal/jap/89/4?ver=pdfcov>

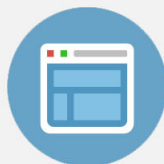
Published by the [AIP Publishing](#)

Advertisement:



Re-register for Table of Content Alerts

Create a profile.



Sign up today!



Lateral oxidation kinetics of AlAsSb and related alloys lattice matched to InP

S. K. Mathis, K. H. A. Lau,^{a)} A. M. Andrews, and E. M. Hall
Materials Department, University of California, Santa Barbara, California 93106

G. Almuneau and E. L. Hu
Electrical and Computer Engineering Department, University of California, Santa Barbara, California 93106

J. S. Speck^{b)}
Materials Department, University of California, Santa Barbara, California 93106

(Received 20 July 2000; accepted for publication 1 November 2000)

The lateral oxidation kinetics of AlAs_{0.56}Sb_{0.44} on InP substrates have been investigated to understand the antimony segregation process during oxidation. Oxidation layers were grown between GaAsSb buffer and cap layers on InP substrates by molecular beam epitaxy. Oxidation temperatures between 325 and 500 °C were investigated for AlAsSb layer thicknesses between 100 and 2000 Å. At low oxidation temperatures ($T_{\text{ox}} \leq 400$ °C), the process is reaction limited with a linear dependence of oxidation depth on time. At intermediate oxidation temperatures ($400 < T_{\text{ox}} < 450$ °C), the oxidation process becomes diffusion limited. At high oxidation temperatures, the oxidation process is termed self-limiting since at 500 °C the process stops entirely after oxidation times on the order of 5 min and distances of 40 μm. It is shown that the antimony float layer lags the oxidation front by a temperature-dependent distance, which suggests that the antimony may change the structure of the oxide at the front and cause self-limiting behavior. The oxidation kinetics of Al_xGa_{1-x}AsSb and Al_xIn_{1-x}AsSb have also been investigated. Antimony segregation is not suppressed during oxidation of Ga-containing layers and AlInAsSb quaternary alloys do not oxidize laterally at measurable rates in the range 400–525 °C. SiN_x cap layers deposited after growth and before oxidation do not affect the Sb segregation or oxidation rate, but do smooth the cap surface by preventing uneven Sb metal segregation to the cap/oxide interface.
 © 2001 American Institute of Physics. [DOI: 10.1063/1.1335825]

INTRODUCTION

Lateral oxidation of III–V semiconductors has provided a unique processing route to creating insulators between epitaxial layers.¹ The oxidation process is selective for Al-bearing III–V compounds and penetrates only a minimal distance (<50 Å) into adjacent Ga- or In-containing layers.² Lateral oxidation of AlGaAs grown on GaAs substrates has been used to electrically isolate GaAs-based field effect transistors, to create current-confinement apertures for vertical cavity lasers (VCSELs), and in the strain relaxation of InGaAs capping layers (lattice-engineered layers).^{3–5} At the InP lattice constant, desirable applications for lateral oxidation include current apertures for long-wavelength VCSELs and the strain relaxation of capping layers for use in devices. However, the two available lattice-matched oxidation materials [Al(As,Sb) and (Al,In)As] both have drawbacks as lateral oxidation layers. AlInAs has a low oxidation rate at high temperature (500–525 °C), leading to material degradation and decreased oxidation selectivity.⁶ AlAsSb oxidizes quickly at low temperature, but produces a bilayer of oxide and antimony metal; the Sb layer typically “floats” to the upper interface between the oxide and semiconductor cap.⁷

Two studies have examined the lateral oxidation of AlAsSb grown on InP substrates in the temperature range 300–400 °C.^{7,8} Blum *et al.* showed that the wet lateral oxidation of AlAsSb forms Al₂O₃ with small amounts of residual arsenic and a continuous antimony layer forming at the interface between the Al₂O₃ and the semiconductor. This “float layer” is a mixture of amorphous and crystalline antimony, as verified by Raman spectroscopy.⁷ The oxide layer is 2%–12% thinner than the original (unoxidized) layer thickness;⁷ however, the continuous antimony layer increases the overall thickness by ~15% and the overall structure has a greater thickness than the original structure.⁸ This is in contrast to lateral oxidation of AlGaAs where the oxidized layer is thinner than the unoxidized layer.² Legay *et al.* reported that the oxidation process is reaction limited (linear dependence of oxidation depth on time) in the temperature range 300–400 °C with an activation energy of 1.2 eV.⁶ Legay *et al.* also reported that there was no change in the lateral oxidation rate with thickness of the oxidation layer for AlAsSb layers either 1.5 μm thick or 500 Å thick.⁸

In this work, we have carried out a comprehensive study of the lateral oxidation kinetics of Al(As,Sb) and associated alloys of (Al,Ga)(As,Sb) and (Al,In)(As,Sb) in an attempt to control the structure of the resulting oxide layer. The role of antimony in the oxidation process was studied to determine whether it is possible to eliminate the float layer. AlAsSb

^{a)}Current Address: Materials Department, Division of Engineering, Brown University, Providence, RI 02912.

^{b)}Electronic mail: speck@mrl.ucsb.edu

TABLE I. Oxidation structure summary. All samples had the structure: 2000 Å GaAsSb/Oxidation layer/2000 Å GaAsSb/InP substrate. Each of the listed samples were grown as separate structures.

Experiment	Samples	General summary of results
(1) AlAsSb thickness study	(i) 100 Å AlAsSb	Oxidation not observed for 100 Å layer; thickness-dependent rate between 200–500 Å; thickness-independent rate between 500–2000 Å; antimony float layer is 20% of oxidation layer thickness
	(ii) 200 Å AlAsSb	
	(iii) 300 Å AlAsSb	
	(iv) 500 Å AlAsSb	
	(v) 1000 Å AlAsSb	
	(vi) 2000 Å AlAsSb	
(2) Al _x Ga _{1-x} AsSb composition study	(i) 2000 Å AlAsSb	Gallium promotes reaction-limited oxidation; 10% gallium slows oxidation to very low rate; antimony float layer remains same thickness
	(ii) 2000 Å Al _{0.98} Ga _{0.02} AsSb	
	(iii) 2000 Å Al _{0.95} Ga _{0.05} AsSb	
	(iv) 2000 Å Al _{0.90} Ga _{0.10} AsSb	
(3) Al _x In _{1-x} As _{1-y} Sb _y composition study	(i) 2000 Å AlAsSb	Oxidation only observed for 0%–5% indium; no oxidation in range 400–520 °C for samples (iii) and (iv)
	(ii) 2000 Å Al _{0.95} In _{0.05} As _{0.60} Sb _{0.40}	
	(iii) 2000 Å Al _{0.76} In _{0.24} As _{0.76} Sb _{0.24}	
	(iv) 2000 Å Al _{0.60} In _{0.40} As _{0.90} Sb _{0.10}	
(4) AlAsSb/GaAsSb superlattice structures	(i) 10×(25 Å GaAsSb, 75 Å AlAsSb)	Antimony float layer same thickness as for AlAsSb; GaAsSb sublayers appears to have internally oxidized
	(ii) 5×(50 Å GaAsSb, 150 Å AlAsSb)	

oxidation was carried out in the range 325–500 °C in a wet N₂ atmosphere. As we will show, the resulting structure of aluminum oxide and antimony float layer were ubiquitous for AlAsSb with or without additions of gallium or indium, with an uneven antimony segregation leading to a surface undulation with a period on the order of ~10 μm.

EXPERIMENTAL PROCEDURE

Lateral oxidation structures were grown by molecular beam epitaxy in a Varian Gen-II system equipped with solid, valved, cracked antimony (Sb₂) and arsenic (As₂). All of the structures reported here consisted of a 2000 Å GaAsSb buffer layer grown on InP followed by the oxidation layer, and capped with another 2000 Å GaAsSb layer. Growth was carried out at a substrate temperature of 500 °C. Arsenic and antimony flux conditions were chosen using group V-induced reflection high energy electron diffraction oscillations according to a previously published method.⁹ Once these fluxes were chosen for GaAs_{0.51}Sb_{0.49} lattice-matched growth, the aluminum growth rate was adjusted to find a condition for AlAs_{0.56}Sb_{0.44} at 500 °C at constant As₂ and Sb₂ flux. X-ray diffraction was used to confirm the composition of both AlAsSb and GaAsSb layers. The GaAsSb/AlAsSb layer compositions were accurate for all samples within ±3% arsenic of the target compositions of GaAs_{0.51}Sb_{0.49} and AlAs_{0.56}Sb_{0.44}. Strain in the (Al,Ga)AsSb layers did not exceed ±0.2%, and therefore both strain and composition variations are minimal in this sample series.

The oxidation layers investigated are summarized in Table I. Four types of oxidation layers were studied: (1) an AlAsSb thickness study, (2) an Al_xGa_{1-x}AsSb composition study, (3) an Al_xIn_{1-x}As_{1-y}Sb_y composition study, and (4) an investigation of AlAsSb/GaAsSb superlattices. Samples in series (1) were grown using the calibrations described above. AlGaAsSb alloys in sample series (2) were grown

using the digital alloy technique for 5% and 10% gallium layers, with sublayers of GaAsSb and AlAsSb (e.g., 1 Å GaAsSb×19 Å AlAsSb for an overall composition of Al_{0.95}Ga_{0.05}AsSb). Al_{0.98}Ga_{0.02}AsSb layers in series (2) were grown by choosing the gallium growth rate to be 10% of that of the aluminum growth rate and repeating alternating layers of (4 Å Al_{0.9}Ga_{0.1}AsSb×16 Å AlAsSb). In series (4), AlAsSb/GaAsSb superlattice oxidation layers were grown with composition 10×(25 Å GaAsSb, 75 Å AlAsSb) and 5×(50 Å GaAsSb, 150 Å AlAsSb). The total aluminum/gallium ratio of the oxidation layers were held constant.

In series (3), layers of AlInAsSb were grown to reduce the proportion of antimony in the oxidation layer while maintaining lattice-matched growth on InP substrates. Growth was carried out at 385 °C to ensure a near-unity sticking coefficient for indium. For these layers only, the substrate temperature was monitored by a thermocouple mounted behind the substrate. It was also determined by atomic force microscopy (AFM) that the smoothest layers of AlInAsSb were grown at 385 °C, with a minimum of 11 Å root mean square roughness. Lattice matching was achieved by growing calibration samples with the target Al:In beam flux ratio. The arsenic flux was set at a constant overpressure and the antimony flux was varied until a lattice-matched condition was found. Three target compositions were grown on separate wafers: Al_{0.60}In_{0.40}As_{0.90}Sb_{0.10}, Al_{0.76}In_{0.24}As_{0.76}Sb_{0.24}, and Al_{0.95}In_{0.05}As_{0.60}Sb_{0.40}, all grown 2000 Å thick with 2000 Å GaAsSb cap and buffer layers.

Uncapped samples were oxidized at temperatures between 325 and 500 °C in a 5 cm tube furnace with N₂ bubbled through deionized water held at 90 °C. Oxidation was performed on freshly cleaved edges as opposed to etched mesas to minimize exposure of the AlAsSb sidewalls to air. Optical microscopy was used to measure the lateral

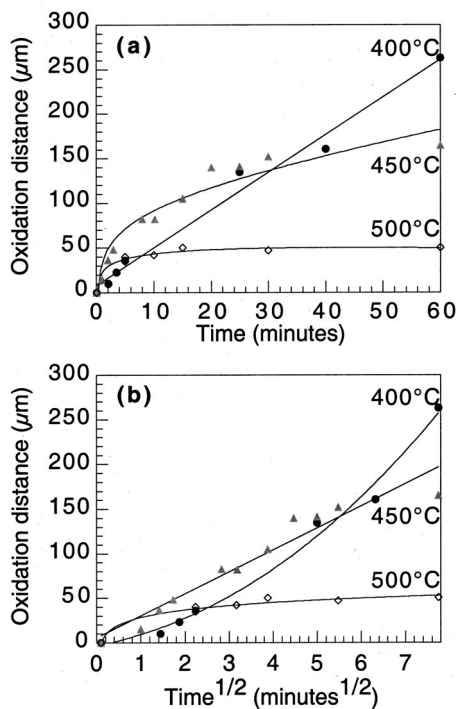


FIG. 1. Oxidation distance as a function of time for 400, 450, and 500 °C. The structure is 2000 Å GaAsSb/2000 Å AlAsSb/2000 Å GaAsSb grown lattice matched to an InP substrate. Oxidation was measured from cleaved edges. In both (a) and (b), the data are fitted as follows: 400 °C with $x \propto t$; 450 °C with $x \propto \sqrt{t}$; and 500 °C with $x \propto \ln(t)$. (a) Up to 400 °C, the oxidation is reaction limited, whereas at 450 °C and higher, it is diffusion limited. At 500 °C, oxidation is self-limiting, and proceeds for ~ 40 – 50 μm after 5 min and stops. (b) Oxidation distance is shown as a function of $t^{1/2}$, which is linear for diffusion-limited samples. At 500 °C, the oxidation rate (and the diffusion constant) approach zero as the oxidation becomes self-limiting.

extent of the oxidation. Scanning electron microscopy (SEM) and AFM were used to characterize the oxidation layer and antimony layer. SEM samples were cleaved cross sections of the oxidized structure observed in a JEOL field emission microscope. To study the effect of a rigid dielectric cap, 0.45 μm silicon nitride was deposited on as-grown samples using a plasma-enhanced chemical vapor deposition system before oxidation, which produces a dense polycrystalline nitride film.

RESULTS

The oxidation distance with time for oxidations carried out at 400, 450, and 500 °C for a 2000 Å GaAsSb/2000 Å AlAsSb/2000 Å GaAsSb/InP sample is shown in Fig. 1(a). Oxidation distance varies linearly with time for temperatures of 400 °C and below. An activation energy of 1.46 eV was measured for reaction-limited oxidation between 325 and 400 °C. At 425–450 °C, lateral oxidation is still reaction limited for short times, but becomes diffusion limited for longer times. The oxidation distance x for long times varies as $x \sim \sqrt{Dt}$, where x is the oxidation distance, D is the diffusion constant, and t is oxidation time. At 500 °C, however, the oxidation process becomes self-limiting since it proceeds linearly for a short distance, and does not proceed any further for longer oxidation times. Figure 1(b) shows the oxidation distance dependence on $t^{1/2}$, which illustrates that lateral ox-

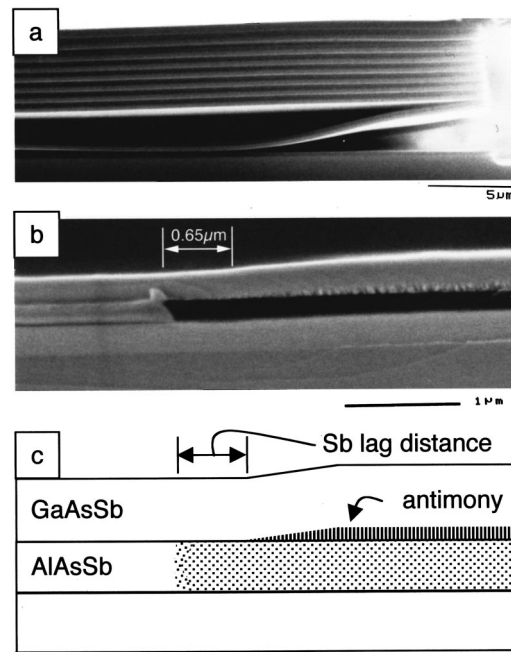


FIG. 2. (a) SEM micrograph of AlAsSb/Al_{0.2}Ga_{0.8}AsSb distributed Bragg reflector test structure after lateral oxidation at 400 °C. The antimony (bright layers) is segregated upward within each oxidation layer to the interface between the oxide (dark layers) and the Al_{0.2}Ga_{0.8}AsSb semiconductor (medium-contrast layers), and the structure delaminates at two Sb/AlO_x interfaces. (b) SEM micrograph of laterally oxidized structure of 2000 Å GaAsSb/2000 Å AlAsSb/2000 Å GaAsSb/InP substrate. The antimony segregation layer lags the oxidation front by 0.65 μm after 1 h oxidation at 400 °C. (c) Schematic of the oxidation layer structure demonstrating the lag between the oxidation front and the leading edge of the antimony float layer.

idation of AlAsSb is diffusion limited at 450 °C. Additionally, it shows that at 500 °C, the diffusion constant (slope) approaches zero for times greater than ~ 5 min.

Antimony segregation is harmful for further sample processing due to the weak bond between the antimony and the oxide layers. Figure 2(a) shows an oxidized GaAsSb/AlAsSb multilayer stack that has fractured at two of the Sb/oxide interfaces. This type of fracture was not observed on single oxidized layers after oxidation. The antimony is also observed to segregate to the upper interface within each of the oxidation layers. A single oxidation layer of 2000 Å AlAsSb is shown in Fig. 2(b) with an oxidation front inclined toward the cap. Both the Sb segregation layer and the cap deformation lag the oxidation front by ~ 0.6 μm . In Fig. 2(c), the antimony layer and oxidation front are shown schematically.

The distance between the oxidation front and the leading edge of the Sb layer depends linearly on oxidation temperature, as shown in Fig. 3(a). However, Fig. 3(b) shows that there is no systematic dependence of the fractional increase in thickness with oxidation temperature for 2000 Å AlAsSb oxidation. The data shown in Fig. 3(b) corresponds to the oxidation depths and times shown in Fig. 1(a). The increase in thickness had no relationship to the oxidation time or depth and therefore these data are not indicated in Fig. 3(b). The fractional increase in thickness is defined as $h_{\text{step}}/h_{\text{AlAsSb}}$ for AFM measurements and as $(h_{\text{oxide}} + h_{\text{Sb}} - h_{\text{AlAsSb}})/h_{\text{AlAsSb}}$ for cross-section SEM measurements, where h refers to layer thickness. In addition, an average

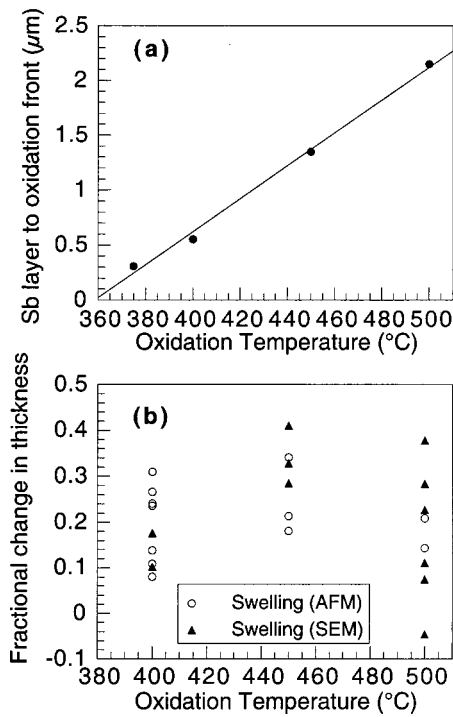


FIG. 3. (a) Distance from oxidation front to antimony segregation layer, measured by cross-section SEM, as a function of oxidation temperature after oxidation for 30 min. The antimony segregation layer lags the oxidation front for each sample, and increases to a maximum measured distance of 2.2 μm at 500 °C. (b) Measured thickness increase across the oxidation front as a function of oxidation temperature. Measurements were made using AFM and cross-section SEM. As the data demonstrate, there is no dependence of total thickness increase on the oxidation temperature. This indicates that antimony is not removed with increasing temperature.

overall layer thickness increase of ~15% was found for all of the structures tested in this study, including AlAsSb layers of different thickness, AlAsSb/GaAsSb superlattices, and AlGaAsSb alloys.

The structure of the antimony layer changed with oxidation temperature. On the surface of the oxidized sample and at oxidation temperatures below 400 °C, raised ridges formed parallel to the oxidation front (in the <110> directions). At 400 °C, peaks appeared that were aligned along both the <110> directions. Figure 4 shows a Nomarski micrograph of the 2000 Å GaAsSb cap surface after lateral oxidation of 2000 Å AlAsSb at 400 °C for 60 min. Morphological order-

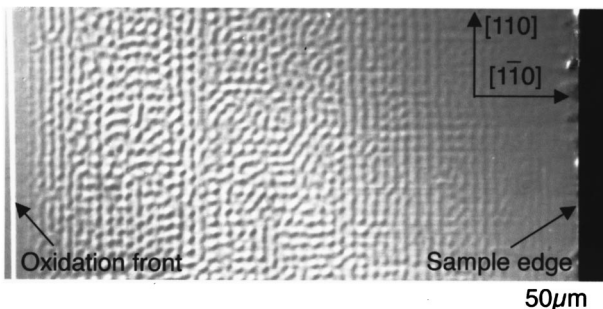


FIG. 4. Optical micrograph of the surface of the same structure as in Fig. 2(b) after oxidation at 400 °C for 1 h. The surface is deformed by peaks spaced at ~5 μm and aligned along the [110] directions.

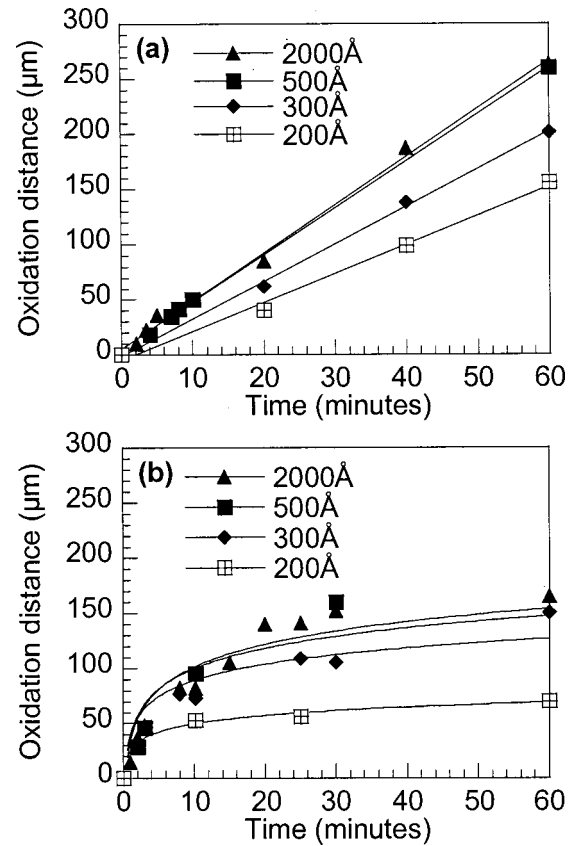


FIG. 5. Effect of layer thickness on oxidation rate. (a) At 400 °C, lateral oxidation is rate limited by the oxidation reaction at the oxidation front. The data show that there is no effect of layer thickness when the layer is thicker than 500 Å, but a decreasing rate is found for thinner layers. A 100 Å thick AlAsSb layer did not oxidize at a measurable rate. (b) At 450 °C, the oxidation is rate limited by diffusion. Layers thinner than 500 Å are also rate limited by diffusion, but with a lower apparent diffusion constant.

ing was apparent in the optical microscope and by AFM. The cap layer was deformed by peaks aligned along the <110> directions and spaced at ~5–10 μm. At 425 °C and above, the surface undulations were still present, but disordered. It is likely that these peaks were caused by local thickening of the antimony metal layer, deforming the top cap.

The effect of AlAsSb layer thickness on the lateral oxidation rate is shown in Fig. 5. The lateral oxidation rate does not have a thickness dependence for layers thicker than 500 Å, whereas layers thinner than 500 Å have decreasing lateral oxidation rates. The oxidation distance varies linearly with time at 400 °C for all four thicknesses shown in Fig. 5(a). A 100 Å thick AlAsSb layer did not oxidize laterally at any temperature in this study. At 450 °C, as shown in Fig. 5(b), oxidation is diffusion limited for all layer thicknesses, but 300 Å and 200 Å thick AlAsSb layers have a lower apparent diffusion constant and therefore do not oxidize as far as thicker layers. At 500 °C, lateral oxidation is self-limiting for all thicknesses.

A thick layer of 0.45 μm SiN_x was deposited on samples of 2000 Å GaAsSb/2000 Å AlAsSb/2000 Å GaAsSb/InP substrate to prevent deformation of the upper cap layer. Silicon nitride capping layers did not affect lateral oxidation rates or the structure of the oxidized samples in these experi-

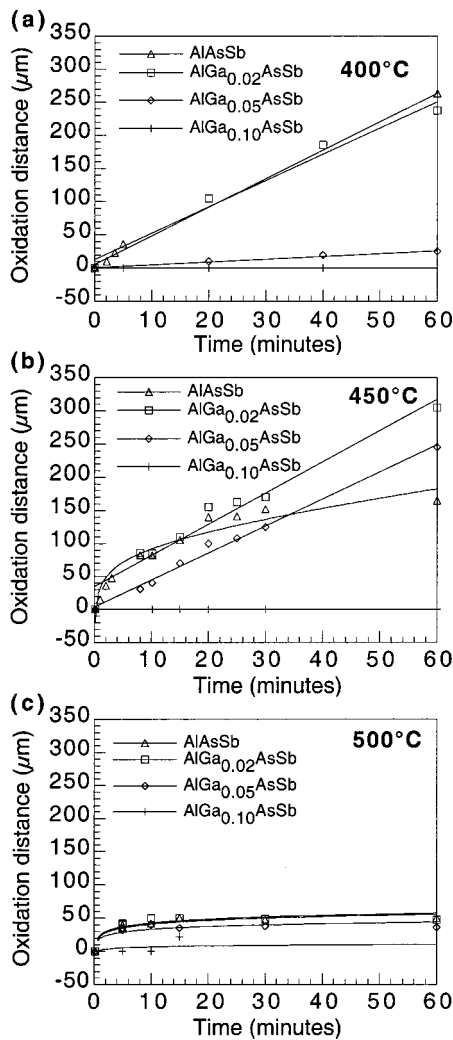


FIG. 6. Oxidation kinetics of $\text{Al}_x\text{Ga}_{1-x}\text{AsSb}$ grown on InP, where $0.90 < x < 1$. Each structure consisted of 2000 Å GaAsSb/2000 Å AlGaAsSb/2000 Å GaAsSb grown lattice matched to an InP substrate. (a) Lateral oxidation of AlGaAsSb at 400 °C is linear with time for 0%, 2%, and 5% gallium, but $\text{Al}_{0.90}\text{Ga}_{0.10}\text{AsSb}$ did not oxidize. (b) Oxidation at 450 °C is parabolic for AlAsSb, but linear for 2%, and 5% gallium. $\text{Al}_{0.90}\text{Ga}_{0.10}\text{AsSb}$ did not oxidize at 450 °C. (c) Self-limiting oxidation was observed for 0%, 2%, 5%, and 10% gallium in AlGaAsSb.

ments. Specifically, the antimony segregation layer was still observed to float to the capping layer/oxide interface. Due to thermal expansion coefficient mismatch and the thickness of the dielectric cap, the SiN_x cracked when the oxidation temperature was raised above 380 °C. However, after the removal of the SiN_x cap layer using a CF_4 plasma, the GaAsSb cap over the oxidized area does not have the periodic undulations seen in Fig. 4.

The lateral oxidation distance with time for 2000 Å thick quaternary $\text{Al}_x\text{Ga}_{1-x}\text{AsSb}$ layers is shown in Figs. 6(a)–6(b). SEM revealed that the antimony float layer is still present in all of the oxidized structures and has the same average thickness at $\sim 20\%$ of the original oxidation layer thickness. In Fig. 6(a), at 400 °C, the oxidation rate for 2% Ga layers is the same as AlAsSb, whereas the 5% and 10% Ga layers oxidized very slowly. At 450 °C in Fig. 6(b), the AlAsSb oxidation becomes diffusion limited with x propor-

tional to $t^{1/2}$, whereas the quaternary alloy oxidation remained reaction limited. In contrast, all of the oxidation layers experienced self-limiting oxidation at 500 °C.

AllInAsSb quaternary layers did not prove useful for lateral oxidation. $\text{Al}_{0.95}\text{In}_{0.05}\text{As}_{0.60}\text{Sb}_{0.40}$ oxidized to a distance of ~ 20 μm at 450 °C after 1 h, but the cap layer height increased by ~ 380 Å, or 19% of the oxidation layer thickness, as measured by AFM. At 400 °C, 5% indium slowed oxidation so that it was not possible to measure the oxidation distance after 1 h. At 500 °C, $\text{Al}_{0.95}\text{In}_{0.05}\text{As}_{0.60}\text{Sb}_{0.40}$ layers also did not oxidize. The two higher indium content layers did not oxidize at 400, 450, 500, or 520 °C for times up to 1 h.

Superlattices of GaAsSb/AlAsSb were also investigated. GaAsSb/AlAsSb oxidation layers of the structure $10 \times (25$ Å GaAsSb, 75 Å AlAsSb) and $5 \times (50$ Å GaAsSb, 150 Å AlAsSb) were grown between 2000 Å GaAsSb cap and buffer layers. After oxidation at 400, 450, and 500 °C, a single antimony float layer had still formed at the upper interface between the oxidation layer and the top GaAsSb cap layer. The GaAsSb interlayers did not prevent antimony segregation as no layered contrast was observed in cross-section SEM.

DISCUSSION

The lateral oxidation kinetics of AlAsSb and AlGaAsSb are similar to AlAs and AlGaAs in temperature, thickness, and composition dependence. Oxidation of AlAs and AlGaAs has been evaluated in terms of the Deal and Grove model, initially formulated for the oxidation of the surface of a silicon substrate.^{10,11} The model describes the time dependence of the oxidized depth by¹¹

$$\frac{x^2}{k_{\text{diffusion}}} + \frac{x}{k_{\text{reaction}}} = t. \quad (1)$$

AlAs oxidation is reaction limited below approximately 350 °C, and becomes diffusion limited at temperatures of 350 °C and above.¹⁰ In contrast, $\text{Al}_{0.98}\text{Ga}_{0.02}\text{As}$ oxidation is reaction limited (linear x vs t) up to 440 °C.¹⁰ Ashby *et al.* have reported that increasing the aluminum content or increasing the oxidation temperature of AlGaAs will favor parabolic oxidation due to the increasing thickness of an As_2O_3 and As-rich zone near the oxidation front.¹⁰ However, it remains an open question whether reactant diffusion to the oxidation front or product diffusion away from the oxidation front is the rate-limiting step in lateral oxidation.

Similar to AlAs and AlGaAs lateral oxidation layers, AlAsSb lateral oxidation becomes diffusion limited at temperatures of ~ 425 °C and higher. When gallium is added to AlAsSb, lateral oxidation is still reaction limited at least up to 450 °C, as shown in Fig. 6(b). GaAsSb oxidizes more slowly than AlAsSb at a constant temperature, and therefore the quaternary AlGaAsSb is more likely to be rate limited by the oxidation reaction. Self-limiting oxidation is found for all AlAsSb and AlGaAsSb layers in this study at 500 °C. The thickness of the antimony metal segregation layer is unchanged by oxidation temperature or the addition of gallium and is proportional to the oxidation layer thickness.

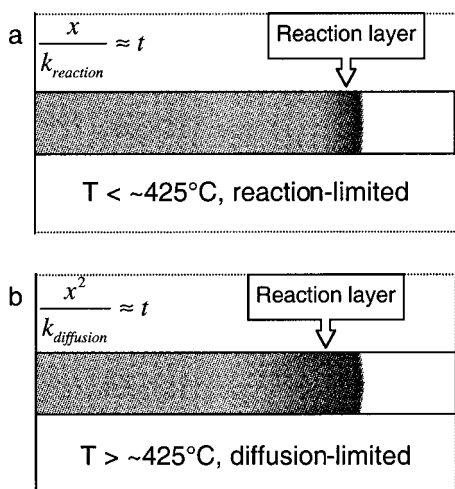


FIG. 7. Proposed lateral oxidation layer structure near the oxidation front. (a) The reaction layer forms as oxidation proceeds with a buildup of reactants during the reaction-limited (low temperature, linear x vs t) regime. (b) The reaction layer becomes wider at higher oxidation temperature, and diffusion-limited lateral oxidation results. Finally, at temperatures of 450 °C and above, self-limiting oxidation dominates, and oxidation stops as the reaction layer becomes impermeable to further diffusion of reactants and/or products.

However, the apparent structure of the antimony layer changes with oxidation temperature. Sb forms an ordered structure with respect to the oxidation front in the reaction-limited regime with raised ridges parallel to the oxidation front. This indicates that there was some mass transport behind the oxidation front at 5–10 μm intervals that resulted in a thickening of the antimony segregation layer. At the highest temperature where reaction-limited oxidation was observed, 400 °C, antimony mass transport took place parallel and perpendicular to the oxidation front. These directions are the $\langle 110 \rangle$ directions of the semiconductor cap and substrate. The temperature may account for the more pronounced surface undulations. For diffusion-limited lateral oxidation at 425 °C and above, however, no ordered surface deformation was observed.

The oxidation rate of AlAsSb depended on layer thickness for layers thinner than ~ 500 Å. Oxidation was prevented for 100 Å layers, while 200 and 300 Å thick layers oxidized slowly. The thickness dependence for AlAsSb was the same as that observed for AlAs, where layers thinner than 500 Å have been shown to have a decreased oxidation rate.¹² AlAs layers thinner than 150 Å have not been observed to oxidize at 400 °C.¹³ It has been suggested by Nane and Coldren that a similar thickness dependence in AlGaAs is due to the effect of interfacial energies producing a “drag” on the oxidation front for thin layers.¹² While our data are consistent with this model, the lateral oxidation front curvature has not been quantified so correlation with the model was not possible.

At temperatures greater than 450 °C, the similarities between AlGaAs and AlGaAsSb end. AlGaAsSb and AlAsSb experience self-limiting oxidation as the temperature is increased and the apparent diffusion constant approaches zero. This indicates a change in the structure or density of the oxidation layer itself at high temperature. In Fig. 7, a sche-

matic of a proposed mechanism for the self-limiting oxidation is shown. This mechanism is analogous to the explanation of diffusion-limited oxidation of AlGaAs in the work of Ashby *et al.* in Ref. 10. At low temperatures, the diffusion of reactants and products through the oxidized layer is fast when compared with the reaction rate. Therefore, any buildup of reactants or products at the oxidation front is minimal. The reactant is water vapor, and the products of AlAsSb oxidation include Al_2O_3 and metallic antimony, which is transported to the upper semiconductor/oxide interface behind the oxidation front. As the temperature is raised, as in Fig. 7(b), the width of a “reaction layer” increases as the reaction rate increases, where reactants or products build up behind the oxidation front. Diffusion across this reaction layer becomes rate limiting. However, at temperatures above ~ 450 °C, the reaction layer changes. It becomes nearly impermeable to diffusion and the oxidation reaction stops.

We propose that the physical change of the reaction layer at the oxidation front is due to an increased solubility of antimony in the Al_2O_3 oxide. At high temperatures, the distance between the antimony float layer and the oxidation front increased, as shown in Fig. 3(a). However, the antimony is not volatile under these conditions, as evidenced by the difficulty in eliminating or thinning the float layer, which is demonstrated by the data in Fig. 3(b). Therefore, the antimony mobility is small when compared with the rate of mass transport through the reaction layer, and the antimony may be increasingly incorporated into the oxidation layer at high temperature. In the study of Rosenberg *et al.* it was shown that dry (O_2) oxidation of antimony metal becomes rate limited at temperatures greater than 350 °C by the desorption of Sb_2O_3 from the surface of the material.¹⁴ This was due to the extremely slow diffusion of reactants or products through Sb_2O_3 in this temperature range. The results of the current study suggest a similar mechanism for self-limiting oxidation where oxidized antimony incorporated into the reaction layer prevents further diffusion of reactants. As a result, the oxidation slows until lateral oxidation is no longer measurable. Whether the oxidation process is rate limited (in the diffusion-limited regime) or self-limited by reactant diffusion or product diffusion has not been determined and is a topic of ongoing study.

When AlInAsSb layers are exposed to the oxidizing atmosphere at high temperatures, a process related to self-limiting oxidation may take place. The AlInAsSb compositions in this study did not oxidize at any temperature. At temperatures below 500 °C, oxidation of high indium content AlInAsSb was not expected, since for ternary AlInAs, temperatures higher than 500 °C are necessary for lateral oxidation.¹⁵ However, at high temperature, the AlInAsSb layers may have experienced self-stopping oxidation so quickly as to prevent a measurable amount of oxidation. In other words, the antimony may have incorporated into the oxide at the beginning of the oxidation process, effectively blocking further oxidation.

SiN_x capping layers are useful in protecting the surface of the thin film during lateral oxidation in two ways. First, they protect the surface in the steam/ N_2 atmosphere. Second, they prevent the formation of Sb-induced surface ripples or

undulations. However, SiN_x layers did not prevent antimony segregation, nor do they change the oxidation rate or kinetics. Finally, due to thermal expansion mismatch between the semiconductor and the dielectric cap, thick ($0.45\ \mu\text{m}$) SiN_x layers can only be used at $380\ ^\circ\text{C}$ and below for long oxidation times. Thinner cap layers must be used at higher oxidation temperatures to prevent fracture of the SiN_x cap.

CONCLUSIONS

This study has demonstrated the effect of antimony on the process of lateral oxidation. AlAsSb lateral oxidation is reaction limited up to $\sim 425\ ^\circ\text{C}$, and then becomes diffusion limited at higher temperatures. The addition of 2%–10% gallium promotes reaction-limited oxidation to temperatures greater than $450\ ^\circ\text{C}$, which is analogous to observations of AlGaAs oxidation. AlAsSb lateral oxidation is self-limited at high oxidation temperature ($>450\ ^\circ\text{C}$) due to the presence of antimony. Self-limiting oxidation may explain why AlInAsSb does not oxidize when significant amounts of indium are added ($\sim 24\%$ and greater). Finally, thin AlAsSb layers were rate limited during oxidation by the same mechanism, but diffusion constants were lower than for thick layers.

Thin AlAsSb oxidation layers and the addition of gallium (AlGaAsSb) do not reduce the thickness of the antimony layer relative to the original oxidation layer thickness. Periodic surface undulations were observed at oxidation temperatures up to $400\ ^\circ\text{C}$ but were absent at higher oxidation temperatures. SiN_x capping layers smoothed the surface of the oxidized structure without changing the oxidation kinetics.

ACKNOWLEDGMENTS

The authors gratefully acknowledge the ongoing support of the Air Force Office of Scientific Research through the

PRET Center at UCSB (Dr. G. Witt, contract monitor), and from the NC A&T State University subcontract under Dr. S. Iyer. This work made use of the MRL Central Facilities supported by the National Science Foundation under Award No. DMR96-32716.

- ¹J. M. Dallesasse, N. Holonyak, Jr., A. R. Sugg, T. A. Richard, and N. El-Zein, *Appl. Phys. Lett.* **57**, 2844 (1990).
- ²K. D. Choquette, K. M. Geib, C. I. H. Ashby, R. D. Twisten, O. Blum, H. Q. Hou, D. M. Follstaedt, B. E. Hammons, D. Mathes, and R. Hull, *IEEE J. Sel. Top. Quantum Electron.* **3**, 916 (1997).
- ³P. Parikh, P. M. Chavarkar, and U. K. Mishra, *IEEE Electron Device Lett.* **18**, 111 (1997).
- ⁴D. L. Huffaker, D. G. Deppe, and K. Kumar, *Appl. Phys. Lett.* **65**, 1611 (1994).
- ⁵P. Chavarkar, L. Zhao, S. Keller, A. Fisher, C. Zheng, J. S. Speck, and U. K. Mishra, *Appl. Phys. Lett.* **75**, 2253 (1999).
- ⁶P. Legay, P. Petit, J. P. Debray, A. Kohl, G. Patriarche, G. Le Roux, M. Juhel, and M. Quillec, *Proceedings of the Conference on InP and Related Materials 1997*, Hyannis, NH, p. 586.
- ⁷O. Blum, K. M. Geib, M. J. Hafich, J. F. Klem, and C. I. H. Ashby, *Appl. Phys. Lett.* **68**, 3129 (1996).
- ⁸P. Legay, P. Petit, G. Le Roux, A. Kohl, I. F. L. Dias, M. Juhel, and M. Quillec, *J. Appl. Phys.* **81**, 7600 (1997).
- ⁹G. Almuneau, E. Hall, S. K. Mathis, and L. A. Coldren, *J. Cryst. Growth* **208**, 113 (2000).
- ¹⁰C. I. H. Ashby, M. M. Bridges, A. A. Allerman, B. E. Hammons, and H. Q. Hou, *Appl. Phys. Lett.* **75**, 73 (1999).
- ¹¹B. E. Deal and A. S. Grove, *J. Appl. Phys.* **36**, 3770 (1965).
- ¹²R. L. Naone and L. A. Coldren, *J. Appl. Phys.* **82**, 2277 (1997).
- ¹³J.-H. Kim, D. H. Lim, K. S. Kim, G. M. Yang, K. Y. Lim, and H. J. Lee, *Appl. Phys. Lett.* **69**, 3357 (1996).
- ¹⁴A. J. Rosenberg, A. A. Menna, and T. P. Turnbull, *J. Electrochem. Soc.* **107**, 196 (1960).
- ¹⁵P. Petit, P. Legay, G. Le Roux, G. Patriarche, G. Post, and M. Quillec, *J. Electron. Mater.* **26**, L32 (1997).